Effect of Source Signal Traffic on Signal Detection for Ambient Backscatter Communication

Yunfei Chen, *Senior Member, IEEE,* Aziz Altaf Khuwaja, Cheng-Xiang Wang, *Fellow, IEEE*

***Abstract*— Ambient backscatter communication (ABC) is a promising method of reducing energy consumption in wireless communications. Previous works on signal detection for ABC often assume that the ambient source signal is always present during backscattering. However, this may not be the case due to the random traffic of the ambient source and the asynchronous operation between source and tag. In this work, the effect of source signal traffic on the detection performance is studied for ABC systems. Firstly, the performances of the existing detectors are analyzed in the presence of source traffic. Both random arrival and random departure are considered. The exponential and uniform traffic models are used. Their bit error rate expressions are obtained by taking advantage of different approximation methods. Then, new detectors taking into account the random traffic models are derived by weighting the samples exponentially or linearly with their arrival times. Numerical results show that the random source traffic could cause large performance degradation to the existing detectors, leading to error floors at small signal-to-noise ratios (SNRs). In particular, the exponential departure causes the largest performance degradation, followed by the uniform arrival and departure. Numerical results also show that the new detectors could have significant performance gains over the conventional detectors in the presence of source traffic. In some case, the gain could be over 3 dB in SNR, and it increases with the sample size and traffic parameters. However, this gain could become negative for large SNRs and small sample sizes due to the use of heuristic detection thresholds.**

***Index Terms*— Ambient backscatter communications, signal traffic, signal detection.**

I. Introduction

With the rapid development of wireless communications, the number of wireless devices has increased dramatically. Consequently, their energy consumption becomes a serious concern. One promising way of reducing the energy consumption in wireless communications is to use existing signals in the ambient environment instead of generating new signals for ambient backscatter communication (ABC) [1] - [7]. In ABC, a radio frequency (RF) tag utilizes signals radiated from the existing wireless systems in the ambient environment, such as Wi-Fi, radio broadcast or mobile, to deliver its information to a reader by controlling the reflection of these signals [1] - [7]. This makes ABC systems passive to save energy but also makes their signal detection very challenging, as the reflected signals that carry useful information could be much weaker than the interference directly from the RF source. Hence, it is crucial to design efficient signal detectors for ABC systems.

Previous works on signal detection for ABC include the following. In [8] and [9], Gaussian approximation was used to derive the maximum likelihood (ML) detectors, where the ambient source signal was assumed to be Gaussian. In [10] and [11], semi-coherent and energy detectors for backscattered signals were derived and their performances were analyzed, where the ambient source signal was assumed to be either Gaussian distributed or phase shift keying (PSK) modulated. Reference [12] applied Manchester coding to the signals before backscattering them for both Gaussian distributed and PSK modulated ambient sources to improve the detection performance. The ML detector was then obtained. Similar to [12], differential encoding and ternary encoding were applied to the original information at the tag followed by ML and maximum *a posteriori* detection in [13] and [14], respectively. In [15], different ML and improved energy detectors, which include the conventional energy and magnitude detectors as special cases, were derived for both Gaussian distributed source and PSK modulated source. In [16], the statistical covariance of the signal was calculated, while in [17], two non-coherent detectors without knowledge of the channel coefficients were derived for single-carrier ABC systems. References [18] - [20] took advantage of the properties of the orthogonal frequency division multiplexing signals to derive non-coherent detectors for multi-carrier systems, while references [21] - [25] derived both coherent and non-coherent detectors for multi-antenna systems, aiming to improve the detection performance by using either multiple carriers or multiple antennas. Other works have used machine learning for signal detection. For example, in [26], deep transfer learning was applied to signal detection for ABC. In [27], constellation learning was used, while in [28], different learning methods, including supervised learning, unsupervised learning, reinforcement learning and deep learning, were discussed for ABC signal detection.

All the aforementioned detectors have good performances

The work of Yunfei Chen is supported in part by the King Abdullah University of Science and Technology Research Funding (KRF) under Award ORA-2021-CRG10-4696 and by EPSRC TITAN (EP/Y037243/1, EP/X04047X/1). The work of Cheng-Xiang Wang was supported by the National Natural Science Foundation of China (NSFC) under Grant 61960206006, the Key Technologies R&D Program of Jiangsu (Prospective and Key Technologies for Industry) under Grants BE2022067 and BE2022067-1, the EU H2020 RISE TESTBED2 project under Grant 872172, and the Research Fund of National Mobile Communications Research Laboratory, Southeast University, under Grant 2024A05. The corresponding author is Yunfei Chen.

Yunfei Chen is with the Department of Engineering, Durham University, Durham, DH1 3LE, UK (e-mail: Yunfei.Chen@durham.ac.uk).

Aziz Altaf Khuwaja is with the Department of Electrical Engineering, Sukkur IBA University, Sukkur, Sindh, Pakistan (e-mail: aziz.khuwaja@iba-suk.edu.pk).

Cheng-Xiang Wang is with National Mobile Communications Research Laboratory, School of Information Science and Engineering, Southeast University, Nanjing 210096, China (e-mail: chxwang@seu.edu.cn).

and are suitable for different applications. However, most have assumed that the ambient source signal is always present during backscattering. This may be true for TV and radio systems with continuous broadcasting but may not be true for Wi-Fi, mobile or radar systems with intermittent traffic. For the latter systems, the ambient source signal may appear or disappear during backscattering, instead of being present all the time, as the backscattering has no control over the activity of the ambient source and the tag is not synchronized with the source. Hence, it is of great interest to examine and improve the performances of the signal detectors for ABC when the ambient source signal is dynamically changing due to traffic. Similar issues have been studied for cognitive radios. For example, in [29] - [34], the effect of the dynamic primary user traffic on the performance of spectrum sensing was studied. However, to the best of the author's knowledge, this issue has not been considered for ABC.

Motivated by the above observations, in this work, the effect of the ambient source signal traffic on the detection of ABC signals is studied. The contributions of this work can be summarized as follows:

- Both exponentially arriving or departing source signals and uniformly arriving or departing source signals are studied. Also, both random Gaussian source and deterministic PSK source are considered.
- The performances of the existing energy detectors and magnitude detectors are analyzed in the presence of source traffic by deriving new bit error rate (BER) expressions. Insights are given to show that the performances of the existing detectors degrade greatly when the ambient source signal is dynamically changing during backscattering. In particular, when the source signal is exponentially departing, the BER reaches error floors very early at small values of signal-to-noise ratio (SNR) to have the largest performance degradation.
- New energy and magnitude detectors using the traffic models of the ambient source signal are derived. Insights are presented to show that the derived new detectors can largely improve the existing detectors in the presence of dynamic source signal by weighting the samples used in the energy and magnitude detectors linearly or exponentially with their arrival times.

The rest of the paper is organized as follows. In Section II, the system model is introduced. In Section III, the performances of the existing energy and magnitude detectors with ambient source signal traffic are analyzed. Section IV discusses the new energy and magnitude detectors by taking the traffic model into account. Numerical results are presented in Section V. Finally, Section VI concludes the paper.

II. System Model

Similar to the previous works on ABC signal detection in [8] - [17], this work also considers a single-carrier and single-antenna ABC system. The ABC system is made of three links: the source-to-tag (ST) link, the tag-to-reader (TR) link and the source-to-reader (SR) link. The ambient source signal is denoted as $s[n]$, where $n = 1, 2, \cdots, N$ index the samples. In the literature, it has been modeled as either a Gaussian random variable with mean zero and variance P_s or a deterministic PSK modulated value as $s[n] = \sqrt{P_s}e^{j\phi_n}$, where ϕ_n is the phase of the n-th bit or sample of the source signal and is unknown. The ambient source signal reaches the reader directly via the SR link but could also be reflected by the tag via the ST and then TR links.

A. Signal Model

If the tag needs to send data to the reader via the TR link, it will reflect the received ambient source signal for bit '1' and will not reflect the received ambient source signal for bit '0'. This is achieved by adjusting the impedance or reflection coefficient at the tag. In this case, the reader will receive both the useful signal from the tag via the TR link and the interfering signal from the ambient source via the SR link so that its received signal is

$$y_1[n] = h_{sr}s[n] + \eta h_{tr}h_{st}s[n] + w[n] \tag{1}$$

for bit '1', where $n = 1, 2, \cdots, N$ index the sequence of the samples, h_{sr}, h_{tr} and h_{st} are the channel coefficients of the SR, TR and ST links, respectively, $s[n]$ is the ambient source signal either Gaussian distributed or PSK modulated, η is the constant reflection coefficient, and $w[n]$ is the additive white Gaussian noise (AWGN) with mean zero and variance σ_w^2. Similarly, for bit '0', its received signal is

$$y_0[n] = h_{sr}s[n] + w[n] \tag{2}$$

where the reflected signal is not there because of bit '0' but the direct interference from the ambient source and the noise remain. The equations in (1) and (2) can also be rewritten as

$$y_1[n] = h_1 s[n] + w[n] \tag{3}$$

and

$$y_0[n] = h_0 s[n] + w[n] \tag{4}$$

for bit '1' and bit '0', respectively, where $h_1 = h_{sr} + \eta h_{tr}h_{st}$ and $h_0 = h_{sr}$. Combining (3) and (4), one has

$$y[n] = hs[n] + w[n] \tag{5}$$

where $h = h_{sr} + d\eta h_{tr}h_{st}$ and d is the data bit of the tag. If the tag transmits bit '1', one has $d = 1$, $h = h_1$ and $y[n] = y_1[n]$ in (5). If the tag transmits bit '0', one has $d = 0$, $h = h_0$ and $y[n] = y_0[n]$ in (5). Note that the signal detector needs to determine whether $d = 1$ or $d = 0$ by using $y[n]$ in (5). Note also that the tag data rate is often much smaller than the source data rate so that d is treated as a constant within the N samples of the ambient source signal $s[n]$, $n = 1, 2, \cdots, N$. However, this also means that the ambient source is more dynamic than the tag so that the ambient source signal $s[n]$ may appear or disappear during backscattering, as the tag and the ambient source are not necessarily synchronized. In the previous works, $s[n] \neq 0$ for $n = 1, 2, \cdots, N$ so that the ambient source signal is always present during backscattering. In our work, the random traffic of $s[n]$ will be considered so that the ambient source signal leaves or arrives during backscattering and part of the N samples will become zero. Next, the traffic models of the ambient source will be described. For later use, define $\sigma_0^2 = |h_0|^2 P_s + \sigma_w^2$ and $\sigma_1^2 = |h_1|^2 P_s + \sigma_w^2$.

B. Traffic Model

Assume that the ambient source signal appears or disappears only once during the backscattering [29] - [34]. If it randomly arrives or becomes active at the end of the n_0-th sample, the source signal becomes $\tilde{s}[n] = 0$ for $n = 1, 2, \cdots, n_0$ and $\tilde{s}[n] = s[n]$ for $n = n_0+1, \cdots, N$, where $n_0 = 0, 1, \cdots, N-1$. In this case, the received signal at the reader is

$$\tilde{y}[n] = h\tilde{s}[n] + w[n]. \tag{6}$$

One sees that the received signal contains only noise when $n = 1, 2, \cdots, n_0$ before the arrival of the source signal. One also sees that the conventional signal in (5) is a special case of (6) when $n_0 = 0$. Two models of source traffic will be studied in this work. If the source traffic follows an exponential distribution, the probability mass function (PMF) of the arrival time n_0 is given by [32] [34]

$$Pr_{EA}\{n_0\} = [1 - e^{-\lambda_a T}]e^{-n_0\lambda_a T}, n_0 = 0, \cdots, N-1 \tag{7}$$

where λ_a is the arrival parameter of the traffic and T is the time interval of each sample. If the source follows a uniform distribution, the PMF of n_0 is given by

$$Pr_{UA}\{n_0\} = \frac{1}{N}, n_0 = 0, \cdots, N-1. \tag{8}$$

Note that the exponential distribution is commonly used in wireless systems. For example, the traffic of primary users often follows the exponential distribution in cognitive radios [39], [40]. Similarly, 3GPP also recommended exponential distribution for the packet arrival time in sensing [41]. On the other hand, the uniform distribution is widely used in Bayesian problems as a non-informative prior, when no knowledge on the source traffic available [42].

Similarly, assuming that the ambient source signal randomly departs or becomes inactive at the end of the n_1-th sample, the source signal becomes $\hat{s}[n] = s[n]$ for $n = 1, 2, \cdots, n_1$ and $\hat{s}[n] = 0$ for $n = n_1 + 1, \cdots, N$, where $n_1 = 1, 2, \cdots, N$. In this case, the received signal is

$$\hat{y}[n] = h\hat{s}[n] + w[n]. \tag{9}$$

The received signal contains only noise when $n = n_1 + 1, \cdots, N$ after the source becomes inactive or the source signal leaves, and the conventional signal in (5) is a special case of (9) when $n_1 = N$. If the source traffic follows an exponential distribution, the PMF of the departure time n_1 is given by [32] [34]

$$Pr_{ED}\{n_1\} = [1 - e^{-\lambda_d T}]e^{-n_1\lambda_d T}, n_1 = 1, \cdots, N \tag{10}$$

where λ_d is the departure parameter of the traffic. If the source follows a uniform distribution, the PMF of n_1 is given by

$$Pr_{UD}\{n_1\} = \frac{1}{N}, n_1 = 1, \cdots, N. \tag{11}$$

Next, these traffic models will be used in Section III to analyze the performances of the existing energy and magnitude detectors and in Section IV to derive new energy and magnitude detectors in the presence of source traffic.

III. Performance Analysis of Existing Detectors With Traffic

A. Gaussian Source

Start with the Gaussian source in this section, where $s[n] \sim \mathcal{CN}(0, P_s)$. The Gaussian assumption stems from the fact that many orthogonal-frequency-division-multiplexing source signals are approximately Gaussian in the time domain [35]. Also, in a complex radio environment, the source could be a sum of many random signals and according to the central limit theorem, the overall signal can be approximated as Gaussian [12]. Therefore, this assumption has been widely used in the previous works too [8] - [17]. In this case, it was derived in [11] that the conventional energy detector is given by

$$Z = \sum_{n=1}^{N} |y[n]|^2 \underset{H_1}{\overset{H_0}{\gtrless}} T_{ED1}, \sigma_0^2 > \sigma_1^2 \tag{12a}$$

$$Z = \sum_{n=1}^{N} |y[n]|^2 \underset{H_1}{\overset{H_0}{\lessgtr}} T_{ED1}, \sigma_0^2 < \sigma_1^2 \tag{12b}$$

with

$$T_{ED1} = N\frac{\sigma_0^2\sigma_1^2}{\sigma_0^2 - \sigma_1^2}\ln\frac{\sigma_0^2}{\sigma_1^2} \tag{13}$$

where H_0 represents the hypothesis that bit '0' has been transmitted, H_1 represents the hypothesis that bit '1' has been transmitted, and σ_0^2 and σ_1^2 are defined as before.

Similarly, the conventional magnitude detector was derived in [15] as

$$R = \sum_{n=1}^{N} |y[n]| \underset{H_1}{\overset{H_0}{\gtrless}} T_{MD1}, \sigma_0^2 > \sigma_1^2 \tag{14a}$$

$$R = \sum_{n=1}^{N} |y[n]| \underset{H_1}{\overset{H_0}{\lessgtr}} T_{MD1}, \sigma_0^2 < \sigma_1^2 \tag{14b}$$

with

$$T_{MD1} = \sqrt{\left[N + \frac{\pi}{4}N(N+1)\right]\frac{\sigma_0^2\sigma_1^2}{\sigma_0^2 - \sigma_1^2}\ln\frac{\sigma_0^2}{\sigma_1^2}}. \tag{15}$$

In both (12) and (14), $y[n]$ is given by (5).

1) Without Traffic: Consider the case without traffic first as a benchmark. In this case, the BER of the conventional detector in (12) was derived in [11] as

$$P_e = \frac{1}{2\Gamma(N)}\left[\gamma\left(N, \frac{T_{ED1}}{\sigma_0^2}\right) + \Gamma\left(N, \frac{T_{ED1}}{\sigma_1^2}\right)\right] \tag{16}$$

for $\sigma_0^2 > \sigma_1^2$ and

$$P_e = \frac{1}{2\Gamma(N)}\left[\Gamma\left(N, \frac{T_{ED1}}{\sigma_0^2}\right) + \gamma\left(N, \frac{T_{ED1}}{\sigma_1^2}\right)\right] \tag{17}$$

for $\sigma_0^2 < \sigma_1^2$, where $\Gamma(\cdot)$ is the Gamma function [36, eq. (8.310.1)], $\gamma(\cdot,\cdot)$ is the lower Gamma function [36, eq. (8.350.1)] and $\Gamma(\cdot,\cdot)$ is the upper Gamma function [36, 8.350.2].

The BER of the conventional magnitude detector was also derived in [15] as

$$P_e \approx \frac{1}{2\Gamma(m)}\left[\gamma\left(m, \frac{mT_{MD1}^2}{[N+\frac{\pi}{4}N(N-1)]\sigma_0^2}\right) + \Gamma\left(m, \frac{mT_{MD1}^2}{[N+\frac{\pi}{4}N(N-1)]\sigma_1^2}\right)\right] \quad (18)$$

for $\sigma_0^2 > \sigma_1^2$ and

$$P_e \approx \frac{1}{2\Gamma(m)}\left[\Gamma\left(m, \frac{mT_{MD1}^2}{[N+\frac{\pi}{4}N(N-1)]\sigma_0^2}\right) + \gamma\left(m, \frac{mT_{MD1}^2}{[N+\frac{\pi}{4}N(N-1)]\sigma_1^2}\right)\right] \quad (19)$$

for $\sigma_0^2 < \sigma_1^2$, where m is determined by solving $\frac{\Gamma(x+0.5)}{\Gamma(x)\sqrt{x}} = \frac{N\sqrt{\pi/4}}{\sqrt{N+N(N-1)\pi/4}}$ for x. The approximation signs in (18) and (19) are due to the use of the Nakagami-m approximation to the distribution of R in (14), as its exact distribution is not available.

2) Random Arrival: In this case, the ambient source signal $s[n]$ randomly arrives at the end of the n_0-th sample. Using $\tilde{y}[n]$ in (6) to replace $y[n]$ in (12), the decision variable of the conventional energy detector becomes

$$\tilde{Z} = \sum_{n=1}^{N}|\tilde{y}[n]|^2 = \sum_{n=1}^{n_0}|w[n]|^2 + \sum_{n=n_0+1}^{N}|hs[n]+w[n]|^2. \quad (20)$$

One sees that, due to the absence of the ambient source signal in the first n_0 samples, only the last $N-n_0$ samples contain useful signal for detection. This may degrade the detection performance. The larger the value of n_0 is, the poorer the performance will be. When $n_0 = N-1$, only the last sample contains useful signal with the worst performance.

Next, we will derive the BER for the conventional energy detector with randomly arriving source using (20). Both the first and second terms of (20) are Gamma distributed but with non-identical parameters. The exact distribution of the sum of two independent Gamma random variables with different parameters is an infinite series whose coefficients need to be calculated iteratively [37]. This is too complicated. We use the Gamma approximation to $\tilde{Z}$ instead by matching its mean and variance to those of a Gamma distribution [38]. Using (20), its means and variances can be derived as

$$\mu_0^{ED1} = \mathrm{E}\{\tilde{Z}|H_0\} = n_0\sigma_w^2 + (N-n_0)\sigma_0^2 \quad (21a)$$

$$V_0^{ED1} = \mathrm{Var}\{\tilde{Z}|H_0\} = n_0\sigma_w^4 + (N-n_0)\sigma_0^4 \quad (21b)$$

$$\mu_1^{ED1} = \mathrm{E}\{\tilde{Z}|H_1\} = n_0\sigma_w^2 + (N-n_0)\sigma_1^2 \quad (21c)$$

$$V_1^{ED1} = \mathrm{Var}\{\tilde{Z}|H_1\} = n_0\sigma_w^4 + (N-n_0)\sigma_1^4. \quad (21d)$$

Thus, the probability density functions (PDFs) of $\tilde{Z}$ can be approximated as

$$f_{\tilde{Z}}(z|H_0) \approx \frac{z^{k_{a0}-1}e^{-\frac{z}{\theta_{a0}}}}{\theta_{a0}^{k_{a0}}\Gamma(k_{a0})}, z>0 \quad (22)$$

and

$$f_{\tilde{Z}}(z|H_1) \approx \frac{z^{k_{a1}-1}e^{-\frac{z}{\theta_{a1}}}}{\theta_{a1}^{k_{a1}}\Gamma(k_{a1})}, z>0 \quad (23)$$

under H_0 and H_1, respectively, where $k_{a0} = (\mu_0^{ED1})^2/V_0^{ED1}$, $\theta_{a0} = V_0^{ED1}/\mu_0^{ED1}$, $k_{a1} = (\mu_1^{ED1})^2/V_1^{ED1}$, $\theta_{a1} = V_1^{ED1}/\mu_1^{ED1}$ from the Gamma approximation [38]. Using (22) and (23) in the conventional energy detector in (12) with $\tilde{Z}$ in (20) as the decision variable, the BER conditioned on n_0 is derived as

$$P_e^{ED1}(n_0) \approx \frac{\gamma(k_{a0}, \frac{T_{ED1}}{\theta_{a0}})}{2\Gamma(k_{a0})} + \frac{\Gamma(k_{a1}, \frac{T_{ED1}}{\theta_{a1}})}{2\Gamma(k_{a1})} \quad (24)$$

for $\sigma_0^2 > \sigma_1^2$ and

$$P_e^{ED1}(n_0) \approx \frac{\Gamma(k_{a0}, \frac{T_{ED1}}{\theta_{a0}})}{2\Gamma(k_{a0})} + \frac{\gamma(k_{a1}, \frac{T_{ED1}}{\theta_{a1}})}{2\Gamma(k_{a1})} \quad (25)$$

for $\sigma_0^2 < \sigma_1^2$. They are functions of the arrival time n_0, because the means and variances of the Gamma distributions in (21) are functions of n_0. The unconditional BER for exponential arrival can be obtained by using (7) as

$$P_e = \sum_{n_0=0}^{N-1} P_e^{ED1}(n_0)[1-e^{-\lambda_a T}]e^{-n_0\lambda_a T} \quad (26)$$

and the unconditional BER for uniform arrival can be obtained by using (8) as

$$P_e = \frac{1}{N}\sum_{n_0=0}^{N-1} P_e^{ED1}(n_0) \quad (27)$$

where $P_e^{ED1}(n_0)$ is given by (24) for $\sigma_0^2 > \sigma_1^2$ and (25) for $\sigma_0^2 < \sigma_1^2$. Note that the value of $P_e^{ED1}(n_0)$ decreases when n_0 decreases, because a smaller n_0 leads to a larger $N-n_0$ and the conventional energy detector has a smaller BER when the sample size is larger. Hence, $n_0 = 0$ has the smallest BER and the same performance as those in (16) and (17) without traffic, which can be verified by letting $n_0 = 0$ in (24) and (25), but $n_0 > 0$ has a larger BER than those in (16) and (17) without traffic. Note also that in (26) the conditional BERs are exponentially weighted while in (27) they are equally weighted, due to the different traffic models used.

For the conventional magnitude detector, when the ambient source signal randomly arrives, the decision variable in (14) becomes

$$\tilde{R} = \sum_{n=1}^{N}|\tilde{y}[n]| = \sum_{n=1}^{n_0}|w[n]| + \sum_{n=n_0+1}^{N}|hs[n]+w[n]|. \quad (28)$$

Again, only the last $N-n_0$ samples contain useful signal for detection. In this case, the first term and the second term of $\tilde{R}$ are sums of n_0 and $N-n_0$ Rayleigh random variables, respectively, which do not have closed-form expressions for their PDFs. Similar to [15], we use the Nakagami-m approximation by matching the mean and variance of $\tilde{R}$ with those of a Nakagami-m distribution. This gives

$$\mu_0^{MD1} = \mathrm{E}\{\tilde{R}|H_0\} = \frac{n_0}{2}\sqrt{\pi\sigma_w^2} + \frac{(N-n_0)}{2}\sqrt{\pi\sigma_0^2} \quad (29a)$$

$$V_0^{MD1} = \mathrm{Var}\{\tilde{R}|H_0\} = n_0(1-\frac{\pi}{4})\sigma_w^2 + (N-n_0)(1-\frac{\pi}{4})\sigma_0^2 \quad (29b)$$

$$\mu_1^{MD1} = \mathrm{E}\{\tilde{R}|H_1\} = \frac{n_0}{2}\sqrt{\pi\sigma_w^2} + \frac{(N-n_0)}{2}\sqrt{\pi\sigma_1^2} \quad (29c)$$

$$V_1^{MD1} = \mathrm{Var}\{\tilde{R}|H_1\} = n_0(1-\frac{\pi}{4})\sigma_w^2 + (N-n_0)(1-\frac{\pi}{4})\sigma_1^2. \quad (29d)$$

Thus, the PDF of $\tilde{R}$ can be approximated as

$$f_{\tilde{R}}(r|H_0) \approx \frac{2m_{a0}^{m_{a0}} r^{2m_{a0}-1}}{\Gamma(m_{a0})\Omega_{a0}^{m_{a0}}} e^{-\frac{m_{a0}}{\Omega_{a0}} r^2}, r > 0 \quad (30)$$

and

$$f_{\tilde{R}}(r|H_1) \approx \frac{2m_{a1}^{m_{a1}} r^{2m_{a1}-1}}{\Gamma(m_{a1})\Omega_{a1}^{m_{a1}}} e^{-\frac{m_{a1}}{\Omega_{a1}} r^2}, r > 0 \quad (31)$$

for H_0 and H_1, respectively, where $\Omega_{a0} = V_0^{MD1} + (\mu_0^{MD1})^2$, $\Omega_{a1} = V_1^{MD1} + (\mu_1^{MD1})^2$, m_{a0} is determined by $\frac{\Gamma(x+0.5)}{\Gamma(x)\sqrt{x}} = \frac{\mu_0^{MD1}}{\sqrt{\Omega_{a0}}}$, and m_{a1} is determined by $\frac{\Gamma(x+0.5)}{\Gamma(x)\sqrt{x}} = \frac{\mu_1^{MD1}}{\sqrt{\Omega_{a1}}}$. Using (30) and (31) in the conventional magnitude detector in (14), the BER conditioned on n_0 is derived as

$$P_e^{MD1}(n_0) \approx \frac{\gamma(m_{a0}, \frac{m_{a0}}{\Omega_{a0}} T_{MD1}^2)}{2\Gamma(m_{a0})} + \frac{\Gamma(m_{a1}, \frac{m_{a1}}{\Omega_{a1}} T_{MD1}^2)}{2\Gamma(m_{a1})} \quad (32)$$

for $\sigma_0^2 > \sigma_1^2$ and

$$P_e^{MD1}(n_0) \approx \frac{\Gamma(m_{a0}, \frac{m_{a0}}{\Omega_{a0}} T_{MD1}^2)}{2\Gamma(m_{a0})} + \frac{\gamma(m_{a1}, \frac{m_{a1}}{\Omega_{a1}} T_{MD1}^2)}{2\Gamma(m_{a1})} \quad (33)$$

for $\sigma_0^2 < \sigma_1^2$. The unconditional BERs for the magnitude detector are similar to (26) and (27), except that $P_e^{ED1}(n_0)$ is replaced by $P_e^{MD1}(n_0)$ in (32) and (33) in this case.

3) Random Departure: For random departure, the ambient source signal $s[n]$ leaves at the end of the n_1-th sample. Using (9), the decision variable of the conventional energy detector in (12) becomes

$$\hat{Z} = \sum_{n=1}^{N} |\hat{y}[n]|^2 = \sum_{n=1}^{n_1} |hs[n]+w[n]|^2 + \sum_{n=n_1+1}^{N} |w[n]|^2. \quad (34)$$

In this case, only the first n_1 samples contain useful signal for detection. The larger the value of n_1 is, the better the performance will be.

Next, we derive the BER of the conventional energy detector with randomly departing source using (34). Again $\hat{Z}$ is a sum of two Gamma random variables with different parameters, whose exact distribution is too complicated. Applying the Gamma approximation, one has the means and variances of $\hat{Z}$ from (34) as

$$\mu_0^{ED2} = \mathrm{E}\{\hat{Z}|H_0\} = n_1\sigma_0^2 + (N-n_1)\sigma_w^2 \quad (35a)$$

$$V_0^{ED2} = \mathrm{Var}\{\hat{Z}|H_0\} = n_1\sigma_0^4 + (N-n_1)\sigma_w^4 \quad (35b)$$

$$\mu_1^{ED2} = \mathrm{E}\{\hat{Z}|H_1\} = n_1\sigma_1^2 + (N-n_1)\sigma_w^2 \quad (35c)$$

$$V_1^{ED2} = \mathrm{Var}\{\hat{Z}|H_1\} = n_1\sigma_1^4 + (N-n_1)\sigma_w^4. \quad (35d)$$

Similarly, using the approximate Gamma distributions of $\hat{Z}$ in the conventional detector in (12) with $\hat{Z}$ in (34) as the decision variable, the BER conditioned on n_1 is derived as

$$P_e^{ED2}(n_1) \approx \frac{\gamma(k_{d0}, \frac{T_{ED1}}{\theta_{d0}})}{2\Gamma(k_{d0})} + \frac{\Gamma(k_{d1}, \frac{T_{ED1}}{\theta_{d1}})}{2\Gamma(k_{d1})} \quad (36)$$

for $\sigma_0^2 > \sigma_1^2$ and

$$P_e^{ED2}(n_1) \approx \frac{\Gamma(k_{d0}, \frac{T_{ED1}}{\theta_{d0}})}{2\Gamma(k_{d0})} + \frac{\gamma(k_{d1}, \frac{T_{ED1}}{\theta_{d1}})}{2\Gamma(k_{d1})} \quad (37)$$

for $\sigma_0^2 < \sigma_1^2$, where $k_{d0} = (\mu_0^{ED2})^2/V_0^{ED2}$, $\theta_{d0} = V_0^{ED2}/\mu_0^{ED2}$, $k_{d1} = (\mu_1^{ED2})^2/V_1^{ED2}$, $\theta_{d1} = V_1^{ED2}/\mu_1^{ED2}$ in this case [38]. The unconditional BER for exponential departure can be obtained by using (10) as

$$P_e = \sum_{n_1=1}^{N} P_e^{ED2}(n_1)[1-e^{-\lambda_d T}]e^{-n_1\lambda_d T} \quad (38)$$

and the unconditional BER for uniform departure can be obtained by using (11) as

$$P_e = \frac{1}{N}\sum_{n_1=1}^{N} P_e^{ED2}(n_1) \quad (39)$$

where $P_e^{ED2}(n_1)$ is given by (36) for $\sigma_0^2 > \sigma_1^2$ and (37) for $\sigma_0^2 < \sigma_1^2$.

For the conventional magnitude detector, when the ambient source signal randomly departs, the decision variable in (14) becomes

$$\hat{R} = \sum_{n=1}^{N} |\hat{y}[n]| = \sum_{n=1}^{n_1} |hs[n]+w[n]| + \sum_{n=n_1+1}^{N} |w[n]|. \quad (40)$$

No closed-form expressions for the PDF of $\hat{R}$ is available. Using the Nakagami-m approximation by matching the mean and variance of $\tilde{R}$ with those of a Nakagami-m distribution, one has

$$\mu_0^{MD2} = \mathrm{E}\{\hat{R}|H_0\} = \frac{n_1}{2}\sqrt{\pi\sigma_0^2} + \frac{(N-n_1)}{2}\sqrt{\pi\sigma_w^2} \quad (41a)$$

$$V_0^{MD2} = \mathrm{Var}\{\hat{R}|H_0\} = n_1(1-\frac{\pi}{4})\sigma_0^2 + (N-n_1)(1-\frac{\pi}{4})\sigma_w^2 \quad (41b)$$

$$\mu_1^{MD2} = \mathrm{E}\{\hat{R}|H_1\} = \frac{n_1}{2}\sqrt{\pi\sigma_1^2} + \frac{(N-n_1)}{2}\sqrt{\pi\sigma_w^2} \quad (41c)$$

$$V_1^{MD2} = \mathrm{Var}\{\hat{R}|H_1\} = n_1(1-\frac{\pi}{4})\sigma_1^2 + (N-n_1)(1-\frac{\pi}{4})\sigma_w^2. \quad (41d)$$

Following a similar procedure to before, the BER conditioned on n_1 is derived as

$$P_e^{MD2}(n_1) \approx \frac{\gamma(m_{d0}, \frac{m_{d0}}{\Omega_{d0}} T_{MD1}^2)}{2\Gamma(m_{d0})} + \frac{\Gamma(m_{d1}, \frac{m_{d1}}{\Omega_{d1}} T_{MD1}^2)}{2\Gamma(m_{d1})} \quad (42)$$

for $\sigma_0^2 > \sigma_1^2$ and

$$P_e^{MD2}(n_1) \approx \frac{\Gamma(m_{d0}, \frac{m_{d0}}{\Omega_{d0}} T_{MD1}^2)}{2\Gamma(m_{d0})} + \frac{\gamma(m_{d1}, \frac{m_{d1}}{\Omega_{d1}} T_{MD1}^2)}{2\Gamma(m_{d1})} \quad (43)$$

for $\sigma_0^2 < \sigma_1^2$, where $\Omega_{d0} = V_0^{MD2} + (\mu_0^{MD2})^2$, $\Omega_{d1} = V_1^{MD2} + (\mu_1^{MD2})^2$, m_{d0} is determined by solving $\frac{\Gamma(x+0.5)}{\Gamma(x)\sqrt{x}} = \frac{\mu_0^{MD2}}{\sqrt{\Omega_{d0}}}$, and m_{d1} is determined by $\frac{\Gamma(x+0.5)}{\Gamma(x)\sqrt{x}} = \frac{\mu_1^{MD2}}{\sqrt{\Omega_{d1}}}$ in this case. The unconditional BERs are similar to (38) and (39), except that $P_e^{ED2}(n_1)$ is replaced by $P_e^{MD2}(n_1)$ in (42) and (43) in this case.

B. PSK Source

If the source is PSK modulated, one has $s[n] = \sqrt{P_s}e^{j\phi_n}$, where ϕ_n is unknown and can be removed by taking the absolute value of the sample. In this case, the conventional energy detector has the same form as (12) but the detection threshold T_{ED1} in (12) is replaced by [11]

$$T_{ED2} = \frac{N\sigma_w^2}{2} + \frac{N}{2} \sqrt{(2\sigma_0^2 - \sigma_w^2)(2\sigma_1^2 - \sigma_w^2)(1 + \frac{2\sigma_w^2 \ln(\frac{2\sigma_0^2 - \sigma_w^2}{2\sigma_1^2 - \sigma_w^2})}{NP_s(\sigma_0^2 - \sigma_1^2)})}. \tag{44}$$

Similarly, the conventional magnitude detector in this case has the same form as (14) but the detection threshold becomes [15]

$$T_{MD2} = \max\{N\frac{k_1p_0 - k_0p_1}{p_0 - p_1} + \frac{Np_0p_1}{p_0 - p_1} \sqrt{(\frac{k_0}{p_0} - \frac{k_1}{p_1})^2 - \frac{p_0 - p_1}{p_0p_1}(\frac{k_1^2}{p_1} - \frac{k_0^2}{p_0} + \frac{2}{N}\ln\frac{p_1}{p_0})}, N\frac{k_1p_0 - k_0p_1}{p_0 - p_1} - \frac{Np_0p_1}{p_0 - p_1} \sqrt{(\frac{k_0}{p_0} - \frac{k_1}{p_1})^2 - \frac{p_0 - p_1}{p_0p_1}(\frac{k_1^2}{p_1} - \frac{k_0^2}{p_0} + \frac{2}{N}\ln\frac{p_1}{p_0})}\} \tag{45}$$

with

$$k_0 = \frac{\sqrt{\pi\sigma_w^2}}{2}L_{\frac{1}{2}}(-|h_0|^2P_s/\sigma_w^2) \tag{46a}$$

$$p_0 = \sigma_w^2 L_1(-|h_0|^2P_s/\sigma_w^2) - k_0^2 \tag{46b}$$

$$k_1 = \frac{\sqrt{\pi\sigma_w^2}}{2}L_{\frac{1}{2}}(-|h_1|^2P_s/\sigma_w^2) \tag{46c}$$

$$p_1 = \sigma_w^2 L_1(-|h_1|^2P_s/\sigma_w^2) - k_1^2 \tag{46d}$$

where $L(\cdot)$ is the Laguerre polynomial.

1) Without Traffic: When the ambient source signal is always present during backscattering, the BER of the conventional energy detector using the detection threshold in (44) was approximated as [11]

$$P_e \approx \frac{1}{2}\left[1 - Q\left(\frac{T_{ED2} - N\sigma_0^2}{\sqrt{N(2|h_0|^2P_s\sigma_w^2 + \sigma_w^4)}}\right)\right] + \frac{1}{2}Q\left(\frac{T_{ED2} - N\sigma_1^2}{\sqrt{N(2|h_1|^2P_s\sigma_w^2 + \sigma_w^4)}}\right) \tag{47}$$

for $\sigma_0^2 > \sigma_1^2$, and

$$P_e \approx \frac{1}{2}\left[1 - Q\left(\frac{T_{ED2} - N\sigma_1^2}{\sqrt{N(2|h_1|^2P_s\sigma_w^2 + \sigma_w^4)}}\right)\right] + \frac{1}{2}Q\left(\frac{T_{ED2} - N\sigma_0^2}{\sqrt{N(2|h_0|^2P_s\sigma_w^2 + \sigma_w^4)}}\right) \tag{48}$$

for $\sigma_0^2 < \sigma_1^2$, where the Gaussian approximation is applied to the distribution of the decision variable Z, as its exact distribution is not available.

For the conventional magnitude detector using the detection threshold in (45), its BER was approximated as [15]

$$P_e \approx \frac{1}{2}\left[1 - Q\left(\frac{T_{MD2} - Nk_0}{\sqrt{Np_0}}\right)\right] + \frac{1}{2}Q\left(\frac{T_{ED2} - Nk_1}{\sqrt{Np_1}}\right) \tag{49}$$

for $\sigma_0^2 > \sigma_1^2$, and

$$P_e \approx \frac{1}{2}\left[1 - Q\left(\frac{T_{ED2} - Nk_1}{\sqrt{Np_1}}\right)\right] + \frac{1}{2}Q\left(\frac{T_{ED2} - Nk_0}{\sqrt{Np_0}}\right) \tag{50}$$

for $\sigma_0^2 < \sigma_1^2$, where again the Gaussian approximation is used as the exact distribution of R is not available, and k_0, p_0, k_1, p_1 are given in (46).

2) Random Arrival: Similar to the Gaussian source case, when the PSK modulated source randomly arrives at the end of the n_0-th sample, using (6), the decision variable of the conventional energy detector in (12) becomes

$$\tilde{Z} = \sum_{n=1}^{N}|\tilde{y}[n]|^2 = \sum_{n=1}^{n_0}|w'[n]|^2 + \sum_{n=n_0+1}^{N}|h\sqrt{P_s} + w'[n]|^2 \tag{51}$$

where $w'[n] = w[n]e^{-j\phi_n}$ is still AWGN with mean zero and variance σ_w^2 and $s[n] = \sqrt{P_s}e^{j\phi_n}$ has been used. Unlike the Gaussian case where the samples are Gaussian distributed with mean zero, the PSK source gives samples following Guassian distributions with a mean of $h\sqrt{P_s}$ from (51). Thus, the first and second terms of $\tilde{Z}$ follow chi-square distributions with different parameters and they don't have closed-form expressions for their PDFs. Applying the Gaussian approximation to $\tilde{Z}$, one has its means and variances as

$$\mu_0^{ED3} = \mathrm{E}\{\tilde{Z}|H_0\} = n_0\sigma_w^2 + (N - n_0)\sigma_0^2 \tag{52a}$$

$$V_0^{ED3} = \mathrm{Var}\{\tilde{Z}|H_0\} = n_0\sigma_w^4 + (N - n_0)(2|h_0|^2P_s\sigma_w^2 + \sigma_w^4) \tag{52b}$$

$$\mu_1^{ED3} = \mathrm{E}\{\tilde{Z}|H_1\} = n_0\sigma_w^2 + (N - n_0)\sigma_1^2 \tag{52c}$$

$$V_1^{ED3} = \mathrm{Var}\{\tilde{Z}|H_1\} = n_0\sigma_w^4 + (N - n_0)(2|h_1|^2P_s\sigma_w^2 + \sigma_w^4) \tag{52d}$$

from which the BER conditioned on n_0 is derived as

$$P_e^{ED3}(n_0) \approx \frac{1}{2}[1 - Q(\frac{T_{ED2} - \mu_0^{ED3}}{\sqrt{V_0^{ED3}}})] + \frac{1}{2}Q(\frac{T_{ED2} - \mu_1^{ED3}}{\sqrt{V_1^{ED3}}}) \tag{53}$$

for $\sigma_0^2 > \sigma_1^2$ and

$$P_e^{ED3}(n_0) \approx \frac{1}{2}[1 - Q(\frac{T_{ED2} - \mu_1^{ED3}}{\sqrt{V_1^{ED3}}})] + \frac{1}{2}Q(\frac{T_{ED2} - \mu_0^{ED3}}{\sqrt{V_0^{ED3}}}) \tag{54}$$

for $\sigma_0^2 < \sigma_1^2$. The unconditional BERs are the same as those in (26) and (27) except that $P_e^{ED1}(n_0)$ in (26) and (27) is replaced by $P_e^{ED3}(n_0)$ in (53) and (54).

For the conventional magnitude detector, when the ambient source signal randomly arrives, the decision variable in (14) becomes

$$\tilde{R} = \sum_{n=1}^{N}|\tilde{y}[n]| = \sum_{n=1}^{n_0}|w'[n]| + \sum_{n=n_0+1}^{N}|h\sqrt{P_s} + w'[n]|. \tag{55}$$

It does not have closed-form expressions for its PDF. Using the Gaussian approximation, one has

$$\mu_0^{MD3} = \mathrm{E}\{\tilde{R}|H_0\} = \frac{n_0}{2}\sqrt{\pi\sigma_w^2} + \frac{(N-n_0)}{2}\sqrt{\pi\sigma_w^2}L_{\frac{1}{2}}(-|h_0|^2P_s/\sigma_w^2) \quad (56a)$$

$$V_0^{MD3} = \mathrm{Var}\{\tilde{R}|H_0\} = n_0(1-\frac{\pi}{4})\sigma_w^2 + (N-n_0)[\sigma_0^2 - \frac{\pi\sigma_w^2}{4}L_{\frac{1}{2}}^2(-|h_0|^2P_s/\sigma_w^2)] \quad (56b)$$

$$\mu_1^{MD3} = \mathrm{E}\{\tilde{R}|H_1\} = \frac{n_0}{2}\sqrt{\pi\sigma_w^2} + \frac{(N-n_0)}{2}\sqrt{\pi\sigma_w^2}L_{\frac{1}{2}}(-|h_1|^2P_s/\sigma_w^2) \quad (56c)$$

$$V_1^{MD3} = \mathrm{Var}\{\tilde{R}|H_1\} = n_0(1-\frac{\pi}{4})\sigma_w^2 + (N-n_0)[\sigma_1^2 - \frac{\pi\sigma_w^2}{4}L_{\frac{1}{2}}^2(-|h_1|^2P_s/\sigma_w^2)] \quad (56d)$$

Thus, the BER conditioned on n_0 is derived as

$$P_e^{MD3}(n_0) \approx \frac{1}{2}[1-Q(\frac{T_{MD2}-\mu_0^{MD3}}{\sqrt{V_0^{MD3}}})]+\frac{1}{2}Q(\frac{T_{MD2}-\mu_1^{MD3}}{\sqrt{V_1^{MD3}}}) \quad (57)$$

for $\sigma_0^2 > \sigma_1^2$ and

$$P_e^{MD3}(n_0) \approx \frac{1}{2}[1-Q(\frac{T_{MD2}-\mu_1^{MD3}}{\sqrt{V_1^{MD3}}})]+\frac{1}{2}Q(\frac{T_{MD2}-\mu_0^{MD3}}{\sqrt{V_0^{MD3}}}) \quad (58)$$

for $\sigma_0^2 < \sigma_1^2$. The unconditional BERs are the same as those in (26) and (27) except that $P_e^{ED1}(n_0)$ in (26) and (27) is replaced by $P_e^{MD3}(n_0)$ in (57) and (58).

3) Random Departure: In this case, since the ambient source signal $s[n]$ leaves at the end of the n_1-th sample, the decision variable of the conventional energy detector in (12) becomes

$$\hat{Z} = \sum_{n=1}^{N}|\hat{y}[n]|^2 = \sum_{n=1}^{n_1}|h\sqrt{P_s}+w'[n]|^2 + \sum_{n=n_1+1}^{N}|w'[n]|^2. \quad (59)$$

Using the Gaussian approximation, the means and variances of (59) are

$$\mu_0^{ED4} = \mathrm{E}\{\hat{Z}|H_0\} = n_1\sigma_0^2 + (N-n_1)\sigma_w^2 \quad (60a)$$

$$V_0^{ED4} = \mathrm{Var}\{\hat{Z}|H_0\} = n_1(2|h_0|^2P_s\sigma_w^2+\sigma_w^4) + (N-n_1)\sigma_w^4 \quad (60b)$$

$$\mu_1^{ED4} = \mathrm{E}\{\hat{Z}|H_1\} = n_1\sigma_1^2 + (N-n_1)\sigma_w^2 \quad (60c)$$

$$V_1^{ED4} = \mathrm{Var}\{\hat{Z}|H_1\} = n_1(2|h_1|^2P_s\sigma_w^2+\sigma_w^4) + (N-n_1)\sigma_w^4. \quad (60d)$$

Similarly, the BER conditioned on n_1 is derived as

$$P_e^{ED4}(n_1) = \frac{1}{2}[1-Q(\frac{T_{ED2}-\mu_0^{ED4}}{\sqrt{V_0^{ED4}}})]+\frac{1}{2}Q(\frac{T_{ED2}-\mu_1^{ED4}}{\sqrt{V_1^{ED4}}}) \quad (61)$$

for $\sigma_0^2 > \sigma_1^2$ and

$$P_e^{ED4}(n_1) = \frac{1}{2}[1-Q(\frac{T_{ED2}-\mu_1^{ED4}}{\sqrt{V_1^{ED4}}})]+\frac{1}{2}Q(\frac{T_{ED2}-\mu_0^{ED4}}{\sqrt{V_0^{ED4}}}) \quad (62)$$

for $\sigma_0^2 < \sigma_1^2$. The unconditional BERs are the same as those in (38) and (39) except that $P_e^{ED2}(n_1)$ in (38) and (39) is replaced by $P_e^{ED4}(n_1)$ in (61) and (62).

For the conventional magnitude detector with random departure, the decision variable in (14) becomes

$$\hat{R} = \sum_{n=1}^{N}|\hat{y}[n]| = \sum_{n=1}^{n_1}|h\sqrt{P_s}+w'[n]| + \sum_{n=n_1+1}^{N}|w'[n]|. \quad (63)$$

Using the Gaussian approximation to $\hat{R}$, one has

$$\mu_0^{MD4} = \mathrm{E}\{\hat{R}|H_0\} = \frac{N-n_1}{2}\sqrt{\pi\sigma_w^2} + \frac{n_1}{2}\sqrt{\pi\sigma_w^2}L_{\frac{1}{2}}(-|h_0|^2P_s/\sigma_w^2) \quad (64a)$$

$$V_0^{MD4} = \mathrm{Var}\{\hat{R}|H_0\} = (N-n_1)(1-\frac{\pi}{4})\sigma_w^4 + n_1[\sigma_0^2 - \frac{\pi\sigma_w^2}{4}L_{\frac{1}{2}}^2(-|h_0|^2P_s/\sigma_w^2)] \quad (64b)$$

$$\mu_1^{MD4} = \mathrm{E}\{\hat{R}|H_1\} = \frac{N-n_1}{2}\sqrt{\pi\sigma_w^2} + \frac{n_1}{2}\sqrt{\pi\sigma_w^2}L_{\frac{1}{2}}(-|h_1|^2P_s/\sigma_w^2) \quad (64c)$$

$$V_1^{MD4} = \mathrm{Var}\{\hat{R}|H_1\} = (N-n_1)(1-\frac{\pi}{4})\sigma_w^4 + n_1[\sigma_1^2 - \frac{\pi\sigma_w^2}{4}L_{\frac{1}{2}}^2(-|h_1|^2P_s/\sigma_w^2)] \quad (64d)$$

and the BER conditioned on n_1 is derived as

$$P_e^{MD4}(n_1) = \frac{1}{2}[1-Q(\frac{T_{MD2}-\mu_0^{MD4}}{\sqrt{V_0^{MD4}}})]+\frac{1}{2}Q(\frac{T_{MD2}-\mu_1^{MD4}}{\sqrt{V_1^{MD4}}}) \quad (65)$$

for $\sigma_0^2 > \sigma_1^2$ and

$$P_e^{MD4}(n_1) = \frac{1}{2}[1-Q(\frac{T_{MD2}-\mu_1^{MD4}}{\sqrt{V_1^{MD4}}})]+\frac{1}{2}Q(\frac{T_{MD2}-\mu_0^{MD4}}{\sqrt{V_0^{MD4}}}) \quad (66)$$

for $\sigma_0^2 < \sigma_1^2$. The unconditional BERs are the same as those in (38) and (39) except that $P_e^{ED2}(n_1)$ in (38) and (39) is replaced by $P_e^{MD4}(n_1)$ in (65) and (66).

IV. Derivation of New Detectors With Traffic

In this section, new detectors will be derived by taking the traffic model of the ambient source into account.

A. Random Arrival

For randomly arriving signals, if the energy detector knows the arrival time of n_0, the decision variable should be $Z(n_0) = \sum_{n=n_0+1}^{N}|y[n]|^2$ by using samples that contain the useful signal only. In practice, the value of n_0 is not known and needs to be removed from the decision variable. If the ambient source signal is exponentially arriving, using the traffic model in (7), the averaged decision variable becomes

$$\bar{Z}_{EA} = \sum_{n_0=0}^{N-1}[1-e^{-\lambda_a T}]e^{-n_0\lambda_a T}Z(n_0) = \sum_{n=1}^{N}[1-e^{-\lambda_a T n}]|y[n]|^2 \quad (67)$$

and the new energy detector becomes

$$\bar{Z}_{EA} = \sum_{n=1}^{N}[1-e^{-\lambda_a T n}]|y[n]|^2 \underset{H_1}{\overset{H_0}{\gtrless}} T_{ED-EA}, \sigma_0^2 > \sigma_1^2 \tag{68a}$$

$$\bar{Z}_{EA} = \sum_{n=1}^{N}[1-e^{-\lambda_a T n}]|y[n]|^2 \underset{H_1}{\overset{H_0}{\lessgtr}} T_{ED-EA}, \sigma_0^2 < \sigma_1^2. \tag{68b}$$

The new decision variable $\bar{Z}_{EA}$ does not require knowledge of n_0. One sees that, unlike the conventional energy detector in (12) that treats all samples equally, the new detector weights the samples exponentially with their arrival times so that the late-arriving samples have larger weights, as they are more likely to contain useful signals. This agrees with intuition.

If the ambient source signal is uniformly arriving, using (8), the average decision variable can be derived as

$$\bar{Z}_{UA} = \sum_{n_0=0}^{N-1}\frac{1}{N}Z(n_0) = \sum_{n=1}^{N}\frac{n}{N}|y[n]|^2 \tag{69}$$

and the new energy detector is

$$\bar{Z}_{UA} = \sum_{n=1}^{N}\tfrac{n}{N}|y[n]|^2 \underset{H_1}{\overset{H_0}{\gtrless}} T_{ED-UA}, \sigma_0^2 > \sigma_1^2 \tag{70a}$$

$$\bar{Z}_{UA} = \sum_{n=1}^{N}\tfrac{n}{N}|y[n]|^2 \underset{H_1}{\overset{H_0}{\lessgtr}} T_{ED-UA}, \sigma_0^2 < \sigma_1^2. \tag{70b}$$

In this case, the weighting coefficient is linear with the arrival time of the sample. Again, late-arriving samples are given more weights.

Similarly, for magnitude detection, when the ambient signal is exponentially arriving, one has

$$\bar{R}_{EA} = \sum_{n=1}^{N}[1-e^{-\lambda_a T n}]|y[n]| \underset{H_1}{\overset{H_0}{\gtrless}} T_{MD-EA}, \sigma_0^2 > \sigma_1^2 \tag{71a}$$

$$\bar{R}_{EA} = \sum_{n=1}^{N}[1-e^{-\lambda_a T n}]|y[n]| \underset{H_1}{\overset{H_0}{\lessgtr}} T_{MD-EA}, \sigma_0^2 < \sigma_1^2 \tag{71b}$$

and when the the ambient signal is uniformly arriving, one has

$$\bar{R}_{UA} = \sum_{n=1}^{N}\tfrac{n}{N}|y[n]| \underset{H_1}{\overset{H_0}{\gtrless}} T_{MD-UA}, \sigma_0^2 > \sigma_1^2 \tag{72a}$$

$$\bar{R}_{UA} = \sum_{n=1}^{N}\tfrac{n}{N}|y[n]| \underset{H_1}{\overset{H_0}{\lessgtr}} T_{MD-UA}, \sigma_0^2 < \sigma_1^2. \tag{72b}$$

Note that the above new detectors are applicable to both the Gaussian source and the PSK source. Note also that, to minimize the BER, the optimal detection threshold needs to be derived by using the PDFs of the decision variables in H_0 and H_1. However, neither the exact nor the approximate PDFs of $\bar{Z}_{EA}$, $\bar{Z}_{UA}$, $\bar{R}_{EA}$, $\bar{R}_{UA}$ are available. Thus, we set $T_{ED-EA} = T_{ED-UA} = T_{ED1}$ and $T_{MD-EA} = T_{MD-UA} = T_{MD1}$ for the Gaussian source, and $T_{ED-EA} = T_{ED-UA} = T_{ED2}$ and $T_{MD-EA} = T_{MD-UA} = T_{MD2}$ for the PSK source. In this case, the new detectors have the same detection thresholds as the conventional detectors. This is a heuristic choice.

B. Random Departure

For randomly departing signals, if the energy detector knows the departure time of n_1, the decision variable should be $Z(n_1) = \sum_{n=1}^{n_1}|y[n]|^2$, where only the samples that contain the useful signal are used. Again, in practice, the value of n_1 is not known and can be averaged out using the traffic model. For exponentially departing ambient source, using (10), the averaged decision variable becomes

$$\begin{aligned}\bar{Z}_{ED} &= \sum_{n_1=1}^{N}[1-e^{-\lambda_d T}]e^{-n_1\lambda_d T}Z(n_1)\\ &= \sum_{n=1}^{N}[e^{-\lambda_d T n} - e^{-\lambda_d T(N+1)}]|y[n]|^2\\ &\approx \sum_{n=1}^{N}e^{-\lambda_d T n}|y[n]|^2\end{aligned} \tag{73}$$

when N is large so that $e^{-\lambda_d T(N+1)}$ is close to zero, and the new energy detector becomes

$$\bar{Z}_{ED} = \sum_{n=1}^{N}e^{-\lambda_d T n}|y[n]|^2 \underset{H_1}{\overset{H_0}{\gtrless}} T_{ED-ED}, \sigma_0^2 > \sigma_1^2 \tag{74a}$$

$$\bar{Z}_{ED} = \sum_{n=1}^{N}e^{-\lambda_d T n}|y[n]|^2 \underset{H_1}{\overset{H_0}{\lessgtr}} T_{ED-ED}, \sigma_0^2 < \sigma_1^2. \tag{74b}$$

In this case, the new detector still weights the samples exponentially with their arrival times but the early-arriving samples have larger weights, as they are more likely to contain useful signals, when the source is randomly leaving.

If the ambient source signal is uniformly departing, the average decision variable can be derived as

$$\bar{Z}_{UD} = \sum_{n_1=1}^{N}\frac{1}{N}Z(n_1) = \sum_{n=1}^{N}\frac{N+1-n}{N}|y[n]|^2 \tag{75}$$

and the new energy detector is

$$\bar{Z}_{UD} = \sum_{n=1}^{N}\tfrac{N+1-n}{N}|y[n]|^2 \underset{H_1}{\overset{H_0}{\gtrless}} T_{ED-UD}, \sigma_0^2 > \sigma_1^2 \tag{76a}$$

$$\bar{Z}_{UD} = \sum_{n=1}^{N}\tfrac{N+1-n}{N}|y[n]|^2 \underset{H_1}{\overset{H_0}{\lessgtr}} T_{ED-UD}, \sigma_0^2 < \sigma_1^2. \tag{76b}$$

In this case, the weighting coefficient is linear with the arrival time of the sample but early-arriving samples are given more weights.

Similarly, for magnitude detection, when the ambient signal is exponentially departing, one has

$$\bar{R}_{ED} = \sum_{n=1}^{N} e^{-\lambda_d T n}|y[n]| \underset{H_1}{\overset{H_0}{\gtrless}} T_{MD-ED}, \sigma_0^2 > \sigma_1^2 \tag{77a}$$

$$\bar{R}_{ED} = \sum_{n=1}^{N} e^{-\lambda_d T n}|y[n]| \underset{H_1}{\overset{H_0}{\lessgtr}} T_{MD-ED}, \sigma_0^2 < \sigma_1^2 \tag{77b}$$

and when the the ambient signal is uniformly departing, one has

$$\bar{R}_{UD} = \sum_{n=1}^{N} \frac{N+1-n}{N}|y[n]| \underset{H_1}{\overset{H_0}{\gtrless}} T_{MD-UD}, \sigma_0^2 > \sigma_1^2 \tag{78a}$$

$$\bar{R}_{UD} = \sum_{n=1}^{N} \frac{N+1-n}{N}|y[n]| \underset{H_1}{\overset{H_0}{\lessgtr}} T_{MD-UD}, \sigma_0^2 < \sigma_1^2. \tag{78b}$$

Again, neither the exact nor the approximate PDFs of $\bar{Z}_{ED}$, $\bar{Z}_{UD}$, $\bar{R}_{ED}$, $\bar{R}_{UD}$ are available. Thus, we set $T_{ED-ED} = T_{ED-UD} = T_{ED1}$ and $T_{MD-ED} = T_{MD-UD} = T_{MD1}$ for the Gaussian source, and $T_{ED-ED} = T_{ED-UD} = T_{ED2}$ and $T_{MD-ED} = T_{MD-UD} = T_{MD2}$ for the PSK source, to have the same detection threshold as the conventional detectors. The Gaussian approximations do not work well in this case, as $\bar{Z}_{EA}$, $\bar{Z}_{UA}$, $\bar{Z}_{ED}$, $\bar{Z}_{UD}$, $\bar{R}_{EA}$, $\bar{R}_{UA}$, $\bar{R}_{ED}$, and $\bar{R}_{UD}$ are weighted sums with each term having different means and variances so that the central limit theorem may not apply.

V. Numerical Results and Discussion

In this section, the performances of the conventional and new detectors are examined. In the examination, the SNR is defined as $\gamma = \frac{P_s}{\sigma_w^2}$ and changes from 0 dB to 30 dB with a step size of 5 dB. The channel coefficients h_{sr}, h_{st} and h_{tr} are complex Gaussian distributed with mean zero and variance σ_{sr}^2, σ_{st}^2 and σ_{tr}^2, respectively, and the signal-to-inference ratio is defined as $\frac{\eta^2 \sigma_{st}^2 \sigma_{tr}^2}{\sigma_{sr}^2}$ and is fixed at 20 dB, unless otherwise stated. A number of 10^4 random values of h_{sr}, h_{st} and h_{tr} are used to average the BERs. For the existing detectors with traffic, their BER performances are calculated by using the expressions derived in Section III, while for the new detectors with traffic, their BER performances are simulated, as their BER expressions are not available. In the figures, 'ED' refers to the energy detector, and 'MD' refers to the magnitude detector.

Figs. 1 - 4 show the performances of the existing energy and magnitude detectors for a Gaussian ambient source with different traffic models. Fig. 1 is for the case when the source signal arrives exponentially during backscattering. From this figure, the performances of both energy and magnitude detectors degrade considerably when the ambient source arrives exponentially. For example, at $\gamma = 30dB$, the energy and magnitude detectors without traffic have a BER of 9×10^{-3}, while the energy detector with exponential arrival has a BER of 2.5×10^{-2} and the magnitude detector with exponential

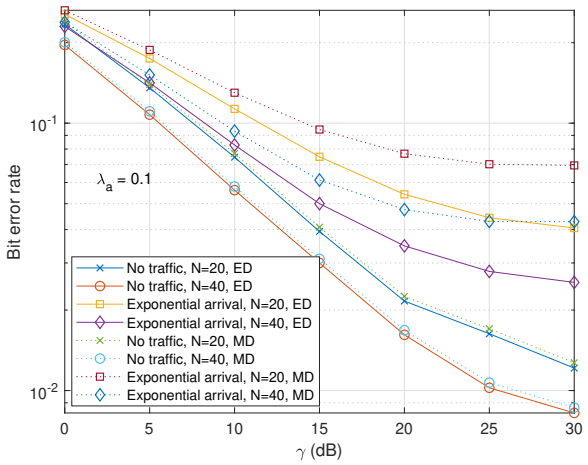

Fig. 1. Performances of existing detectors with exponentially arriving Gaussian source for different N when $\lambda_a = 0.1$.

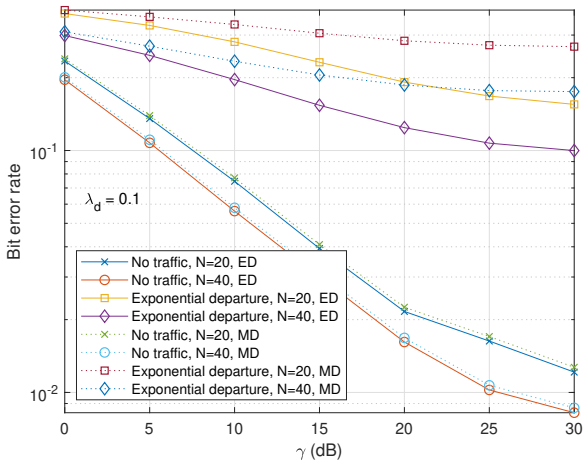

Fig. 2. Performances of existing detectors with exponentially departing Gaussian source for different N when $\lambda_d = 0.1$.

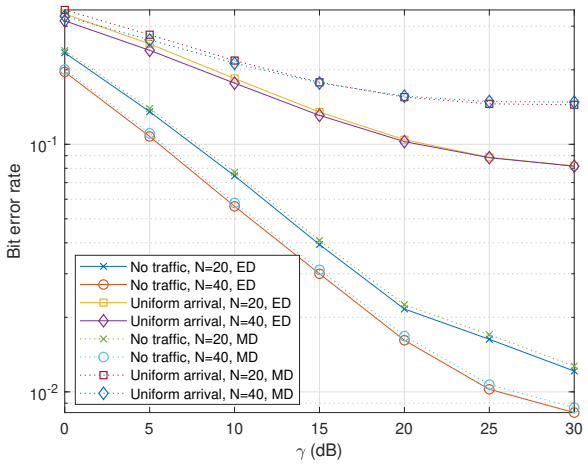

Fig. 3. Performances of existing detectors with uniformly arriving Gaussian source for different N.

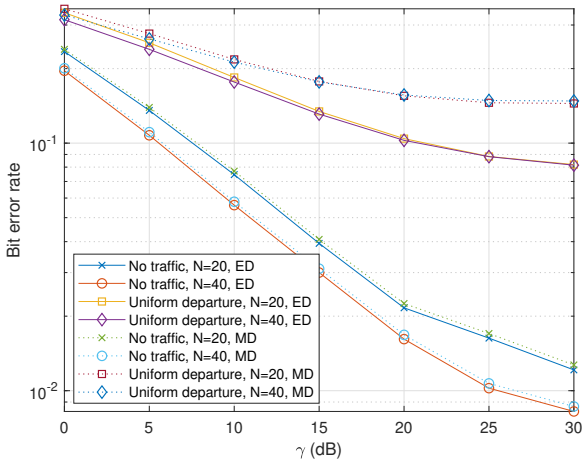

Fig. 4. Performances of existing detectors with uniformly departing Gaussian source for different N.

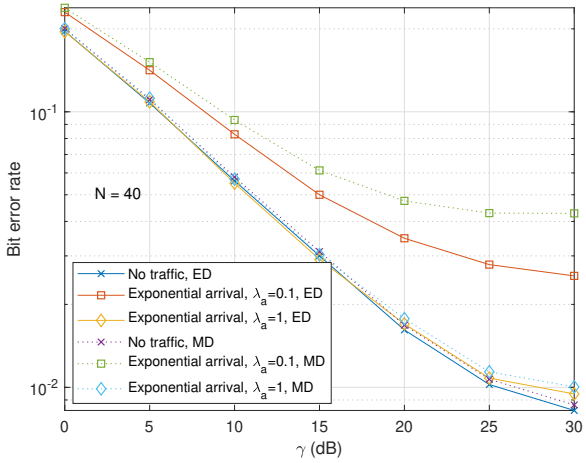

Fig. 5. Performances of existing detectors with exponentially arriving Gaussian source for different λ_a when $N = 40$.

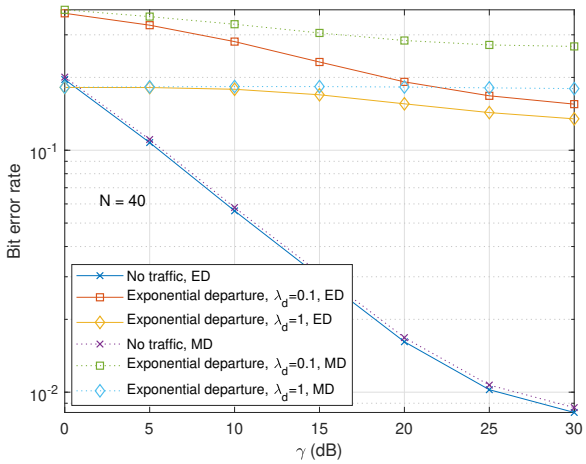

Fig. 6. Performances of existing detectors with exponentially departing Gaussian source for different λ_d when $N = 40$.

arrival has a BER of 4×10^{-2}, when $N = 40$. Thus, the source traffic has significant impact on the detection performance. Also, the conventional energy and magnitude detectors have very similar performances when there is no traffic but this is not true any more when the source is exponentially arriving. At the BER of 4×10^{-2}, the two detectors almost have a performance difference of 10 dB, when $N = 40$. One also sees that the magnitude detector degrades more and reaches error floors earlier than the energy detector, when N increases in this case.

Fig. 2 shows the case of exponential departure. Similar observations can be made. Again, the detection performances degrade considerably in the presence of exponential departure and the performance difference between energy detector and magnitude detector with traffic is much larger than that without traffic. Moreover, in this case, the performance degradation caused by the source traffic is much larger than that in the case of exponential arrival. Thus, an exponentially departing source is more damaging to the detection performance than an exponentially arriving source. This can be explained by comparing (26) and (38) as an example. Both BERs in (26) and (38) are sums of N terms. For the exponential departure in (38), when n_1 increases, due to the exponential weighting factor of $e^{-n_1\lambda_d T}$, only the first few terms in (38) are dominant. In these terms, since the effective sample size (number of samples containing useful signal) n_1 is small, the BER $P_e^{ED2}(n_1)$ is large. Thus, the overall BER for exponential departure is large. For the exponential arrival in (26), when n_0 increases, due to the exponential weighting factor of $e^{-n_0\lambda_a T}$, again only the first few terms in (26) are dominant. However, in these terms, since the effective sample size $N - n_0$ is large, the BER $P_e^{ED1}(n_0)$ is small. Thus, the overall BER for exponential arrival is small. One sees that the BERs of the conventional detectors with exponential departure change very little when the SNR increases from 0 dB to 30 dB, or they reach the error floor at very small SNRs.

Figs. 3 and 4 show the detection performances with uniform traffic. Although uniform arrival is different from uniform departure statistically, mathematically their BER expressions are similar. This can be found by comparing (27) and (39) as an example. Hence, their BER performances are very similar to each other by comparing Figs. 3 and 4. Also, the uniform traffic has a larger impact than the exponential arrival traffic but a smaller impact than the exponential departure traffic on the detection performance by comparing Fig. 3 with Fig. 1 and Fig. 2, respectively. This is because of the removal of the exponential weighting factors in the sums of (26) and (38) compared with (27) and (39). Another interesting observation is that the sample size has little impact on the detection performance for the same detector with uniform traffic, especially at large SNRs.

Figs. 5 and 6 show the effects of the traffic parameters on the detection performance. One sees that λ_a has a significant impact on the detection performance. Specifically, the detection performance degrades dramatically as λ_a decreases from 1 to 0.1 but when $\lambda_a = 1$, the conventional detectors with and without traffic have very similar performances and only differ at large SNRs. On the other hand, the detection performance still degrades dramatically as λ_d decreases from 1 to 0.1, even when $\lambda_d = 1$. Thus, when the source is exponentially

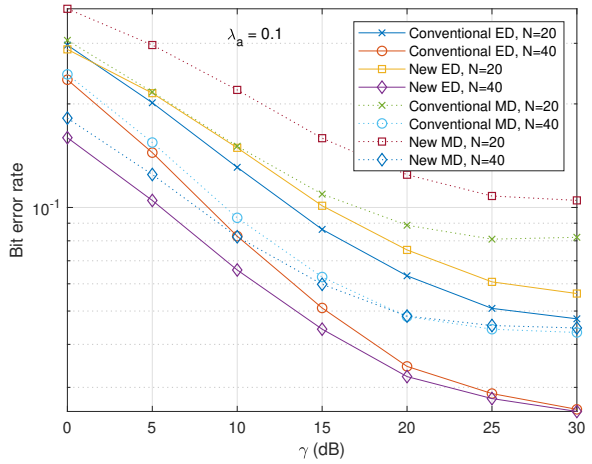

Fig. 7. Comparison of new and existing detectors with exponentially arriving Gaussian source for different N when $\lambda_a = 0.1$.

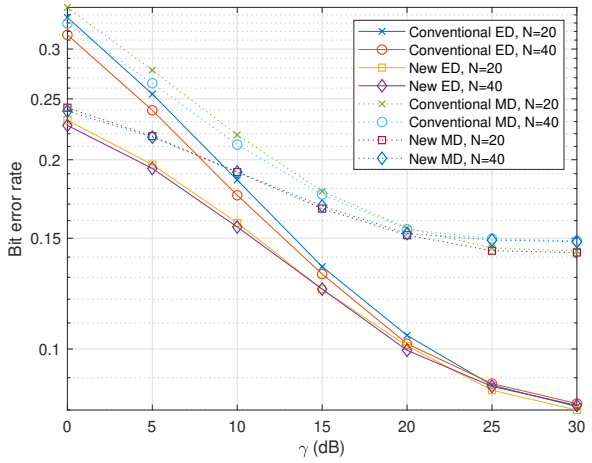

Fig. 8. Comparison of new and existing detectors with uniformly arriving Gaussian source for different N.

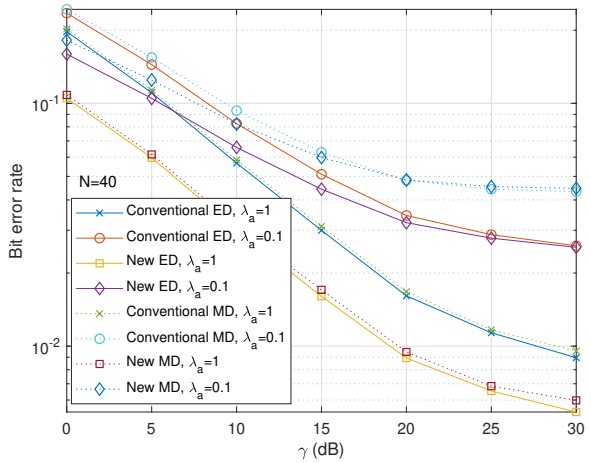

Fig. 9. Comparison of new and existing detectors with exponentially arriving Gaussian source for different λ_a when $N = 40$.

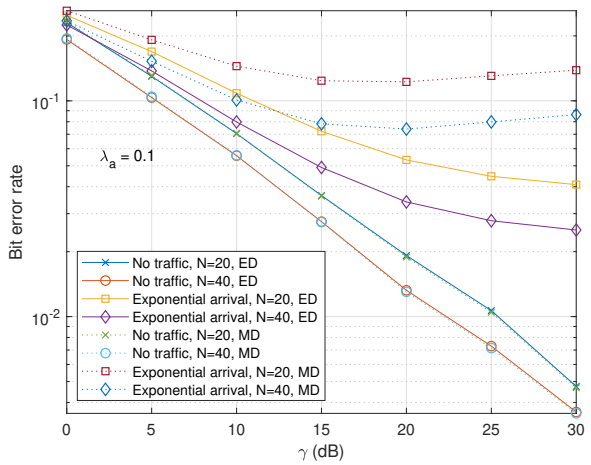

Fig. 10. Performances of existing detectors with exponentially arriving PSK source for different N when $\lambda_a = 0.1$.

departing, the detection performances are very poor in all the cases considered, which agrees with the observation from Fig. 2. Similar observations can be made for other cases. Hence, in the following, results for exponential departure are not shown to save space.

Figs. 7 - 9 compare the performances of the existing detectors with those of the newly derived detectors in Section IV. For the exponential arrival, one sees from Fig. 7 that the new detectors can have considerable performance gains over the conventional detectors. For example, at a BER of 10^{-1}, the new energy detector has a performance gain of around 3 dB over the conventional energy detector, when $N = 40$. This gain diminishes as the SNR increases and could become a loss for large SNR and small values of N. This is because the new detectors use the same detection thresholds as the conventional detectors, instead of their optimum detection thresholds. The optimum detection threshold for the new detector could be obtained by finding the exact distributions of (67) and (73), calculating the error probabilities using (68) and (74), and then minimizing the error probabilities with respect to the detection thresholds. However, this is not possible due to the difficulty in finding the exact distributions of (67) and (73). In this case, the conventional detection threshold is used, leading to a large performance loss, especially at large SNR and small N. For the uniform arrival, one sees from Fig. 8 that the new detectors always outperform the conventional detectors for different values of SNR and N and that the performance gain increases as the SNR decreases. One also sees from Fig. 9 that the new detectors in this case always outperform the conventional detectors and that the performance gain increases when λ_a increases from 0.1 to 1. In fact, at $\lambda_a = 1$, the performance gain remains large even at large SNRs.

Figs. 10 - 12 show the performances of the existing detectors for the PSK source with random traffic. Again, the source traffic degrades the detection performance considerably, especially when N is small, λ_a is small, or the SNR is large. Also, the performance difference between energy and magnitude detectors is increased with traffic. The performance degradation caused by uniform arrival is larger than that caused by exponential arrival. These agrees with the observations for the Gaussian source. Also, comparing Fig. 10 with Fig. 1, one sees

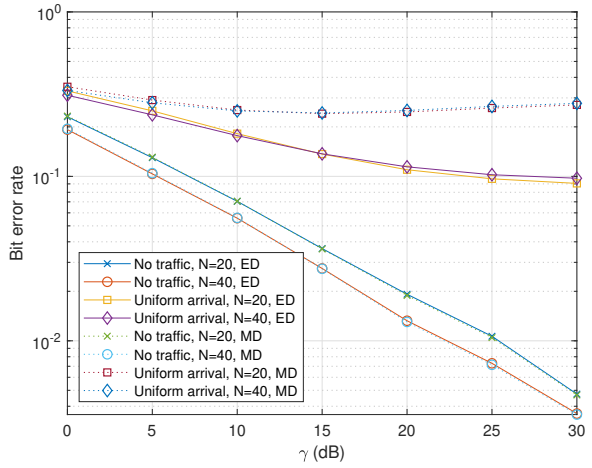

Fig. 11. Performances of existing detectors with uniformly arriving PSK source for different N.

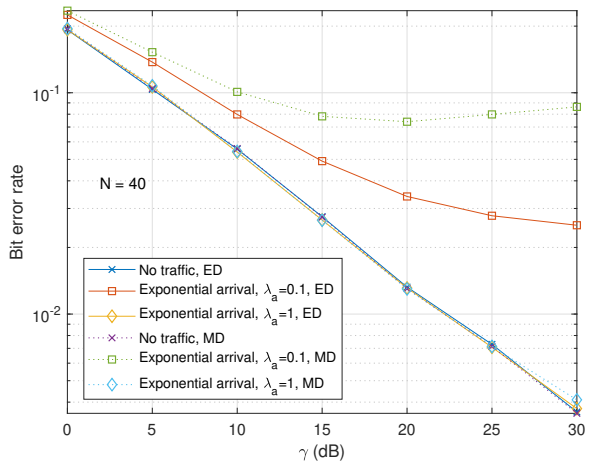

Fig. 12. Performances of existing detectors with exponentially arriving PSK source for different λ_a when $N = 40$.

that the source traffic leads to larger performance degradation for the PSK source than for the Gaussian source.

Figs. 13 - 15 compare the new and conventional detectors in the presence of random ambient PSK source. Similar observations to those from Figs. 7 - 9 for the Gaussian source can be made. The new detectors also outperform the conventional detectors when $N = 40$, the SNR is small or λ_a increases. This is only for the new detectors using the non-optimized detection thresholds. When the detection thresholds are optimized, the performance gain is expected to further increase. Fig. 16 compares different approximations and the simulation. The upper part compares Gamma approximation with simulation, where the markers represent the approximation and the solid lines represent the simulation. One sees that they agree with each other very well, showing the accuracy of the approximation. The lower part compares Gamma approximation and Nakagami approximation with the Gaussian approximation for the Gaussian source, where the markers represent results from Gamma or Nakagami approximations while the solid lines represent results from Gaussian approximation. Again, they are indistinguishable from each other. Similar comparisons can

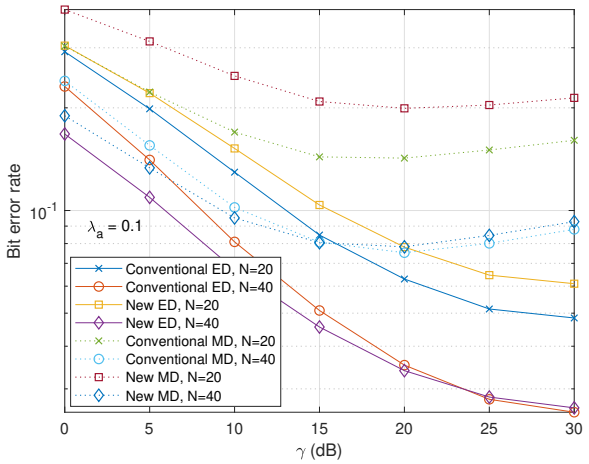

Fig. 13. Comparison of new and existing detectors with exponentially arriving PSK source for different N when $\lambda_a = 0.1$.

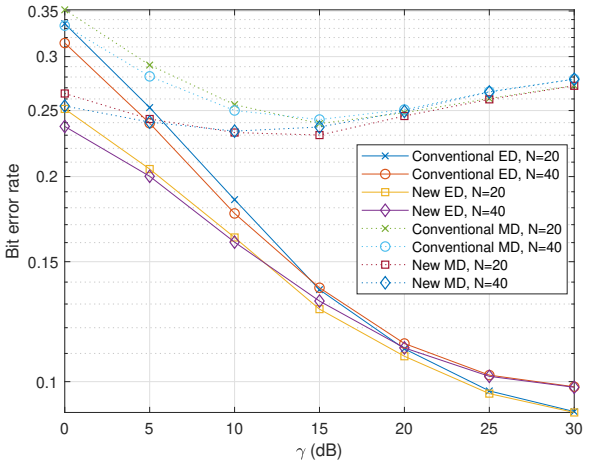

Fig. 14. Comparison of new and existing detectors with uniformly arriving PSK source for different N.

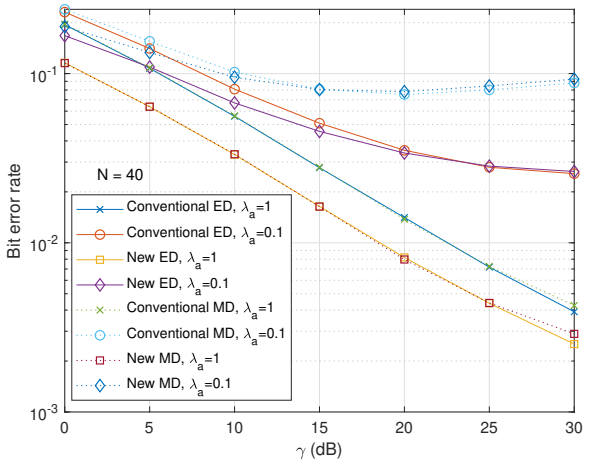

Fig. 15. Comparison of new and existing detectors with exponentially arriving PSK source for different λ_a when $N = 40$.

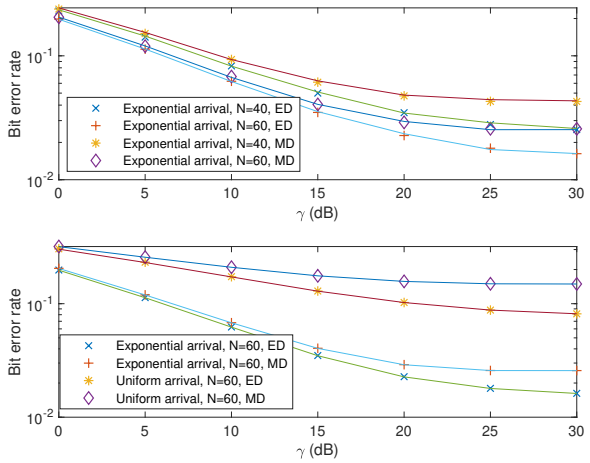

Fig. 16. Comparison of different approximations and simulation for Gaussian source.

also be made for other cases but due to the length restriction, they are not shown here.

Note that the case without traffic is used as a benchmark and therefore most equations in this case are from the literature. However, in the cases with traffic, both the conditional and unconditional BERs are new, as one has to consider the traffic in the derivation of means and variances. They are not straightforward extensions of the case without traffic. For example, (20) becomes a sum of two Gamma random variables and their exact distribution is not Gamma any more. Moreover, Gamma approximation is only a statistical tool used to analyze the BER performances and is not the novelty of the work.

Note also that in (12) and (14) as well as in other detectors, values of σ_0^2 and σ_1^2 are required. These values can be estimated using training symbols, as described in [11, Section IV] or [12, Section III]. To save space, they are not repeated here. Similarly, the traffic model parameters λ_a and λ_d are also required. They can be obtained from traffic modelling using measurements [39] - [41].

VI. Conclusion

The effect of source signal traffic on the performances of existing energy and magnitude detectors for ABC systems has been studied for both exponential and uniform random models. The performance degradation caused by different traffic models has been examined for different values of sample sizes, SNRs and traffic parameters. New detectors accounting for the source traffic models have also been derived. Numerical results have shown that the performance degradation caused by random traffic could be very significant. In particular, for exponentially departing ambient source, the BER of the existing detectors reaches an error floor at very small SNRs. For other traffic models, the performance degradation is determined by the sample size, the traffic parameters and the SNR. Also, the PSK source is more damaging to the detection performance than the Gaussian source. Numerical results have also shown that the new detectors outperform the conventional detectors in all the cases for the uniform traffic models. They also outperforms the conventional detectors for the exponential arrival model in certain cases but could become worse than the conventional detectors when the sample size is small or the SNR is large. Future works will focus on the derivation of the optimal detection threshold for the new detectors as well as their extension to multi-carrier or multi-antenna systems to improve the performances of the new detectors.

References

[1] V. Liu, A. Parks, V. Talla, S. Gollakota, D. Wetherall, and J. R. Smith, "Ambient backscatter: wireless communication out of thin air," *Proc. ACM SIGCOMM Conf.*, pp. 39 - 50, Hong Kong, Aug. 2013.

[2] B. Kellogg, A. Parks, S. Gollakota, J. R. Smith, and D. Wetherall, "Wi-Fi backscatter: Internet connectivity for RF-powered devices," *Proc. ACM SIGCOMM Conf.*, pp. 607 - 618, Chicago, IL, USA, Aug. 2014.

[3] A. N. Parks, A. Liu, S. Gollakota, and J. R. Smith, "Turbocharging ambient backscatter communication," *Proc. ACM SIGCOMM Conf.*, pp. 619 - 630, Chicago, IL, USA, Aug. 2014.

[4] D. Bharadia, K. Joshi, M. Kotaru, and S. Katti, "BackFi: high throughput WiFi backscatter," *Proc. ACM Conf. Special Interest Group Data Commun.*, pp. 283 - 296, London, U.K., Aug. 2015.

[5] B. Kellogg, V. Talla, S. Gollakota, and J. R. Smith, "Passive Wi-Fi: Bringing low power to Wi-Fi transmissions," *Proc. ACM SIGCOMM*, pp. 607–618, Chicago, IL, USA, Aug. 2014.

[6] C. Yang, J. Gummeson, and A. Sample, "Riding the airways: ultra-wideband ambient backscatter via commercial broadcast systems," *Proc. IEEE Conf. Comput. Commun. (INFOCOM)*, pp. 1 - 9, Atlanta, USA, May 2017.

[7] N. V. Huynh, D. T. Hoang, X. Lu, D. Niyato, P. Wang, and D. I. Kim, "Ambient backscatter communications: a contemporary survey," *IEEE Commun. Surveys and Tutorials.*, vol. 20, no. 4, pp. 2889 - 2922, 4th Quarter, 2018.

[8] G. Wang, F. Gao, Z. Dou, and C. Tellambura, "Uplink detection and BER analysis for ambient backscatter communication systems," *Proc. IEEE Global Commun. Conf. (GLOBECOM)*, pp. 1 - 6, San Diego, CA, USA, Dec. 2015.

[9] K. Lu, G. Wang, F. Qu, and Z. Zhong, "Signal detection and BER analysis for RF-powered devices utilizing ambient backscatter," *Proc. 2015 Int. Conf. on Wireless Commun. & Signal Processing (WCSP)*, Nanjing, China, Oct. 2015.

[10] G. Wang, F. Gao, R. Fan, and C. Tellambura, "Ambient backscatter communication systems: detection and performance analysis," *IEEE Trans. Commun.*, vol. 64, no. 11, pp. 4836 - 4846, Nov. 2016.

[11] J. Qian, F. Gao, G. Wang, S. Jin, and H. Zhu, "Semi-coherent detection and performance analysis for ambient backscatter system," *IEEE Trans. Commun.*, vol. 65, no. 12, pp. 5266 - 5279, Dec. 2017.

[12] Q. Tao, C. Zhong, H. Lin, and Z. Zhang, "Symbol detection of ambient backscatter systems with Manchester coding," *IEEE Trans. Wireless Commun.*, vol. 17, no. 6, pp. 4028 - 4038, Jun. 2018.

[13] J. Qian, F. Gao, G. Wang, S. Jin, and H. Zhu, "Noncoherent detections for ambient backscatter system," *IEEE Trans. Wireless Commun.*, vol. 16, pp. 1412 - 1422, no. 3, Mar. 2017.

[14] Y. Liu, G. Wang, Z. Dou, Z. Zhong, "Coding and detection schemes for ambient backscatter communication systems," *IEEE Access*, vol. 5, pp. 4947 - 4953, 2017.

[15] Y. Chen, W. Feng, "Novel signal detectors for ambient backscatter communications in Internet of Things applications," *IEEE Internet of Things J.*, vol. 11, pp. 5388 - 5400, Feb. 2024.

[16] T. Zeng, G. Wang, Y. Wang, Z. Zhong, and C. Tellambura, "Statistical covariance based signal detection for ambient backscatter communication systems," *Proc. 2016 IEEE 84th Vehicular Technology Conference (VTC-Fall)*, Montreal, Canada, Sept. 2016.

[17] S. Guruacharya, X. Lu and E. Hossain, "Optimal non-coherent detector for ambient backscatter communication system," *IEEE Trans. Veh. Technol.*, vol. 69, no. 12, pp. 16197 - 16201, Dec. 2020.

[18] G. Yang, Y.-C. Liang, R. Zhang, and Y. Pei, "Modulation in the air: backscatter communication over ambient OFDM carrier," *IEEE Trans. Commun.*, vol. 66, no. 3, pp. 1219 - 1233, Mar. 2018.

[19] D. Darsena, "Noncoherent detection for ambient backscatter communications over OFDM signals," *IEEE Access*, vol. 7, pp. 159415 - 159425, 2019.

[20] M.A. ElMossallamy, M. Pan, R. Jäntti, K.G. Seddik, G. Li, and Z. Han, "Noncoherent backscatter communications over ambient OFDM signals," *IEEE Trans. Commun.*, vol. 67, no. 5, pp. 3597 - 3611, May 2019.

[21] C.-H. Kang, W.-S. Lee, Y.-H. You, and H.-K. Song, "Signal detection scheme in ambient backscatter system with multiple antennas," *IEEE Access*, vol. 5, pp. 14543 - 14547, Jul. 2017.
[22] Q. Tao, C. Zhong, X. Chen, H. Lin, and Z. Zhang, "Maximum-eigenvalue detector for multiple antenna ambient backscatter communication systems," *IEEE Trans. Veh. Technol.*, vol. 68, pp. 12411 - 12415, Dec. 2019.
[23] W. Liu, S. Shen, D.H.K. Tsang, R. Murch, "Enhancing ambient backscatter communication utilizing coherent and non-coherent space-time codes," *IEEE Trans. Wireless Commun.*, vol. 20, pp. 6884 - 6897, Oct. 2021.
[24] C. Chen, G. Wang, H. Guan, Y.-C. Liang, and C. Tellambura, "Transceiver design and signal detection in backscatter communication systems with multiple-antenna tags," *IEEE Trans. Wireless Commun.*, vol. 19, no. 5, pp. 3273 - 3288, May 2020.
[25] G. Yang, Q. Zhang, Y.-C. Liang, "Cooperative ambient backscatter communictions for green internet-of-things," *IEEE Internet of Things Journal*, vol. 5, pp. 116 - 1130, Apr. 2018.
[26] C. Liu, Z. Wei, D.W.K. Ng, J. Yuan, Y.-C. Liang, "Deep transfer learning for signal detection in ambient backscatter communications," *IEEE Trans. Wireless Commun.*, vol. 20, pp. 1624 - 1638, Mar. 2021.
[27] Q. Zhang, H. Guo, Y.-C. Liang, X. Yuan, "Constellation learning-based signal detection for ambient backscatter communication systems," *IEEE J. Select. Areas in Commun.*, vol. 37, pp. 452 - 463, Feb. 2019.
[28] U.S. Toro, B.M. ElHalawany, A.B. Wong, L. Wang, K. Wu, "Machine-learning-assisted signal detection in ambient backscatter communication networks," *IEEE Network*, vol. 35, pp. 120 - 125, Nov./Dec. 2021.
[29] L. Tang, Y. Chen, E.L. Hines, M.-S. Alouini, "Effect of primary user traffic on sensing-throughput tradeoff for cognitive radios," *IEEE Trans. Wireless Commun.*, vol. 10, pp. 1063 - 1068, Apr. 2011.
[30] S. MacDonald, D.C. Popescu, O. Popescu, "Analyzing the performance of spectrum sensing in cognitive radio systems with dynamic PU activity," *IEEE Communications Lett.*, vol. 21, pp. 2037 - 2040, Sept. 2017.
[31] M. Deng, B.-J. Hu, X. Li, "Adaptive weighted sensing with simultaneous transmission for dynamic primary user traffic," *IEEE Trans. Commun.*, vol. 65, pp. 992 - 1004, Mar. 2017.
[32] N.C. Beaulieu, Y. Chen, "Improved energy detectors for cognitive radios with randomly arriving or departing primary users,"' *IEEE Signal Processing Lett.*, vol. 17, pp. 867 - 870, Oct. 2010.
[33] W.L. Chin, J.M. Li, H.H. Chen, "Low-complexity energy detection for spectrum sensing with random arrivals of primary users," *IEEE Trans. Veh. Technol.*, vol. 65, pp. 947 - 952, Feb. 2016.
[34] J. Wang, R. Chen, J. Huang, F. Shu, Z. Chen, G. Min, "Multiple-antenna spectrum sensing method with random arrivals of primary users," *IEEE Trans. Veh. Technol.*, vol. 67, pp. 8978 - 8983, Sept. 2018.
[35] S. Wei, D. L. Goeckel, and P. A. Kelly, "Convergence of the complex envelope of bandlimited OFDM signals," *IEEE Trans. Info. Theory*, vol. 56, pp. 4893–4904, Oct. 2010.
[36] I.S. Gradshteyn, I.M. Ryzhik, *Tables of Integrals, Series and Products*, 6th Ed. Academic Press: London, 2000.
[37] P.G. Moschopoulos, "The distribution of the sum of independent Gamma random variables," *Ann. Inst. Statist. Math.*, vol. 37, pp. 541 - 544, 1985.
[38] S. Covo and A. Elalouf, "A novel single-gamma approximation to the sum of independent gamma variables, and a generalization to infinitely divisible distributions," *Electronic J. of Statistics*, vol. 8, pp. 894 - 926, 2014.
[39] D. Willkomm, S. Machiraju, J. Bolot, and A. Wolisz, "Primary users in cellular networks: A large-scale measurement study," in *Proc. of the IEEE Symposia on New Frontiers in Dynamic Spectrum Access Networks (DySPAN)*, Oct. 2008
[40] Y. Chen, H.S. Oh, "A survey of measurement-based spectrum occupancy modeling for cognitive radios," *IEEE Commun. Sur. Tut.*, vol. 18, pp. 848 - 859, 2016.
[41] "Study on provision of low-cost machine-type communications (MTC) user equipments (UEs) based on LTE," 3GPP, Sophia Antipolis, France, Rep. TR 36.888, Jun. 2013.
[42] M. Taboga, "Uninformative prior", Lectures on probability theory and mathematical statistics. Kindle Direct Publishing. Online appendix. https://www.statlect.com/fundamentals-of-statistics/uninformative-prior, 2021.